Supplement of Weather Clim. Dynam., 6, 505–520, 2025
https://doi.org/10.5194/wcd-6-505-2025-supplement

Supplement of

Characteristics and dynamics of extreme winters in the Barents Sea in a changing climate

Katharina Hartmuth et al.

Correspondence to: Katharina Hartmuth (katharina.hartmuth@env.ethz.ch)

S1 Correlations between precursor variables

	P	H_S	H_L	R_S	R_L
T	+0.61	+0.53	–0.17	+1.00	+0.89
P		–0.35	–0.89	+0.64	+0.17
H_S			+0.74	+0.50	+0.86
H_L				–0.21	+0.30
R_S					+0.87

	P	H_S	H_L	R_S	R_L
T	+0.66	+0.74	+0.19	–0.59	+0.90
P		–0.02	–0.61	–1.00	+0.26
H_S			+0.80	+0.11	+0.96
H_L				+0.68	+0.61
R_S					–0.18

Table S1. Correlation between surface parameters in region BS (see Sect. 2.1 in the main paper) for DJF in S2000 (left) and S2100 (right).

	P	H_S	H_L	R_S	R_L
T	+0.05	+0.21	+0.36	–1.59	+0.01
P		+0.33	+0.28	–1.64	+0.09
H_S			+0.06	–0.39	+0.10
H_L				+0.89	+0.31
R_S					–1.05

Table S2. Change in correlation between S2000 and S2100.

S2 Daily variability of surface parameters (substructure)

We extend our analysis of seasonal anomalies in surface parameters in different extreme season clusters (see Sects. 4.1 and 5.1 in the main paper) by a more detailed investigation of the substructure of such winters, i.e., the daily variability of surface parameter anomalies, by conducting several case studies. This analysis complements the results shown in Hartmuth et al. (2022, HA2022) who performed similar case studies for present-day extreme winters in the ERA5 dataset. One objective here is to investigate the diversity in extreme winters in region BS (see Sect. 2.1 in the main paper), which has been inhibited using a relatively short record of reanalysis data in HA2022. We further aim to validate the ability of the CESM1 model to represent similar extreme seasons as analyzed by HA2022 in the ERA5 reanalysis. We therefore first investigate the substructure of six extreme winters in BS, whereby always two seasons are part of the same extreme seasons cluster (see Sect. 2.3 in the main paper). While winters from the same cluster are expected to show a similar substructure, large differences between different clusters can be assumed as the clusters feature strongly different seasonal anomalies in the precursor variables, as shown in Sects. 4.1 and 5.1 in the main paper. Note that daily-mean anomalies are calculated similarly to seasonal anomalies as described in Sect. 2.1 in the main paper with the temporal mean being a daily mean instead of a seasonal mean.

S2.1 S2000

S2.1.1 Cluster 1: DJF 1993/94 (member 008) and DJF 1996/97 (member 090)

We first analyze the substructure of two winters in cluster 1, winters 1993/94 in ensemble member 008 (CS1) and 1996/97 in ensemble member 090 (CS2). The analysis of daily-mean values in the key surface parameters shows almost continuously

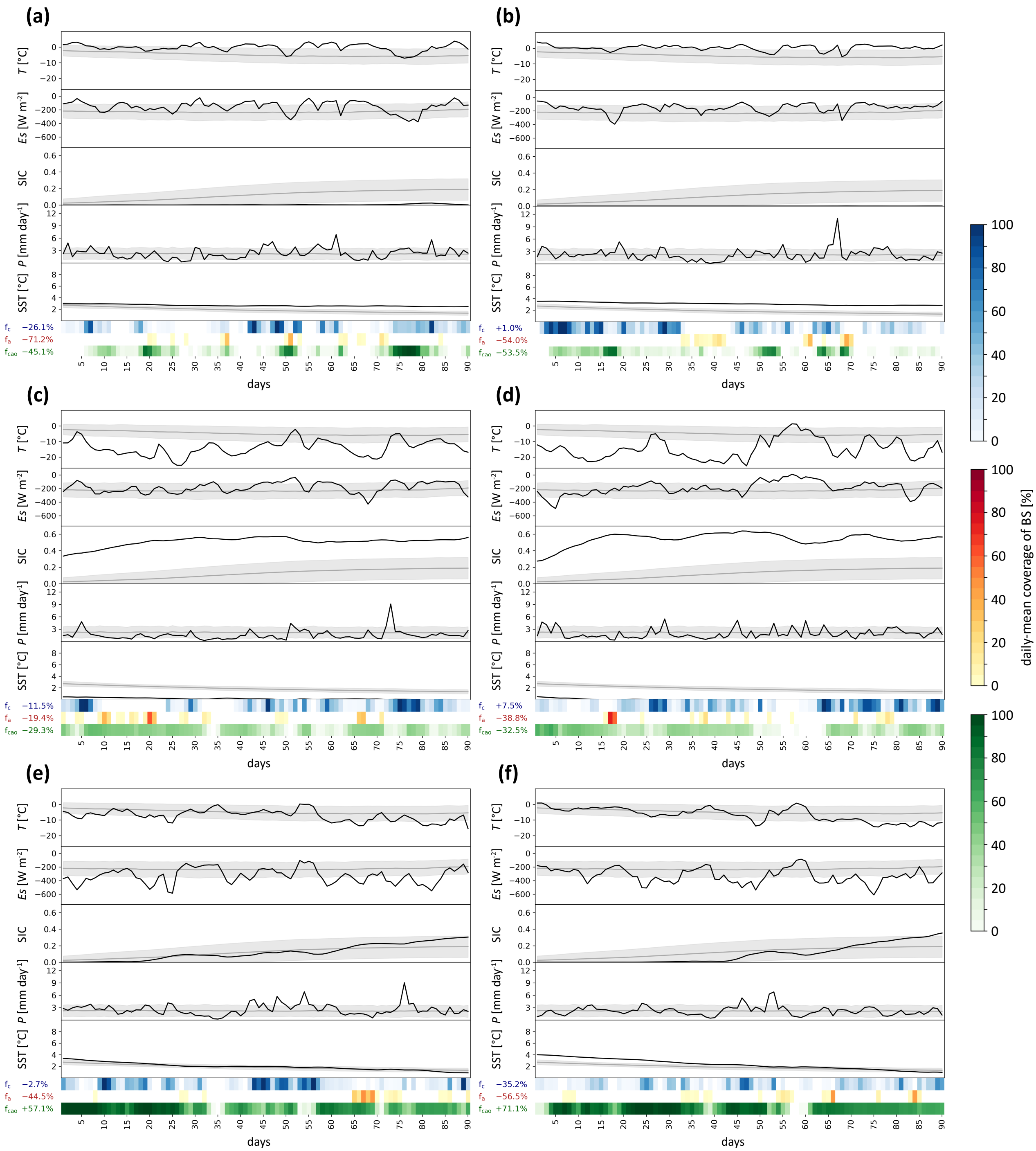

Figure S1. Time series of daily-mean (a, f) T (in °C), (b, g) E_S (in W m^{-2}), (c, h) SIC, (d, i) P (in mm day^{-1}), and (e, j) SST (in °C) averaged for BS in selected extreme winters in S2000 (black lines) for (a) CS1, (b) CS2; (c) CS3, (d) CS4, (e) CS5, and (f) CS6. The climatology is shown by grey lines. Grey shading shows the standard deviation of daily-mean anomalies in all winter seasons of all S2000 members relative to the respective climatology. Blue, orange, and green heatmaps at the bottom of each panel show the daily-mean coverage of BS by cyclones, anticyclones, and CAOs, respectively (the darker the color the higher the coverage). Relative, spatially-averaged frequency anomalies of f_c ($f_{c,clim} = 0.28$), f_a ($f_{a,clim} = 0.04$), and f_{CAO} ($f_{CAO,clim} = 0.42$) are given in %. The horizontal axis indicates days since the start of the season with day 1 corresponding to 01 December.

positive daily-mean T^*, which are correlated with periods of persistent positive anomalies in E_S in both winters (Fig. S1a, b). Notably, daily-mean T values often exceed the range given by one standard deviation, which underlines the unusualness of both winters. The persistence of relatively warm surface temperatures can be associated with persistent positive daily-mean anomalies in SST and a lack of sea ice formation at the same time. In both winters, almost no sea ice has formed until the end of February. Despite the anomaly in open ocean exposure, both winters are characterized by a clear deficit of CAOs (green heatmap in Fig. S1). As the frequency in passing cyclones is only slightly or not reduced at all compared to climatology (blue heatmap in Fig. S1), such a reduction in f_{CAO} is possibly associated with an anomalous cyclone pathway in these winters that is discussed in Sect. 4.2 in the main paper.

S2.1.2 Cluster 2: DJF 1998/99 (member 059) and DJF 1993/94 (member 072)

A detailed analysis of the winters 1998/99 in ensemble member 059 (CS3) and 1993/94 in ensemble member 072 (CS4) shows that the strongly negative T^* shown for cluster 2 (see Fig. 2b in the main paper) results from several persistent periods of daily-mean T values well below the climatology (Fig. S1c, d). These periods, which are occurring for example between days 7 and 45 in CS3, are further characterized by below-average precipitation and can be associated with a lack of cyclone activity in BS, while in the same period the occurrence of anticyclones likely further enhances surface cooling (orange heatmap in Fig. S1). In addition, large and continuous positive anomalies in SIC and concurrent negative anomalies in SST that already exist at the beginning of both winters are likely to facilitate the persistent cold conditions. Whereas on average sea ice formation in BS starts at the beginning of December, both winters already feature a sea ice coverage of more than 25 % at this time. Such a reduction in open ocean area is consistent with a reduction of f_{CAO} in both winters, as by default CAOs are not defined over sea ice (see Sect. 2 in the main paper).

S2.1.3 Cluster 3: DJF 1999/00 (member 008) and DJF 1997/98 (member 052)

While the previously shown winters are partially characterized by pronounced anomalies in surface air temperatures, the winters 1999/00 in member 008 (CS5) and 1997/98 in member 052 (CS6) exhibit relatively small seasonal-mean T anomalies in BS. Interestingly, both winters show persistent negative anomalies in daily-mean T during February, resulting in an overall slightly negative T^* (Fig. S1e, f). These periods coincide with a positive SIC anomaly, which, however, only develops during the second half of both winters. The unusualness of winters in cluster 3 results from a strongly negative ${E_S}^*$. The timeseries of both case study winters reveal recurrent events of strongly negative daily E_S anomalies, which can be linked to CAOs that facilitate strong oceanic heat loss in the form of upward H_S and H_L. At least in the beginning of both winters, upward surface heat fluxes are further enhanced by a negative anomaly in daily-mean SIC. While both winters are characterized by a relative lack of anticyclones, CS6 also features a reduction in f_c.

As expected from their position in the PCA biplot, the three pairs of case studies representing three distinct clusters of extreme winters differ strongly from each other. Winters in cluster 1, which feature a positive T^* and ${E_S}^*$, are characterized by a lack of sea ice and at the same time a reduced frequency in CAOs. In contrast, winters in cluster 2 feature negative seasonal-mean anomalies in T and P. These winters are characterized by an unusually high SIC in BS and concurrent relatively low SST values throughout the season, which facilitates the persistence of cold and dry conditions. Finally, winters in cluster 3 are characterized by negative seasonal-mean anomalies in E_S. The persistent occurrence of CAOs results in several episodes of enhanced heat loss into the atmosphere, causing strong negative daily-mean E_S anomalies and a rapid growth of SIC in BS.

S2.2 S2100

S2.2.1 Cluster 1: DJF 2094/95 (member 052) and DJF 2097/98 (member 071)

Winters 2094/95 in ensemble member 052 (CS7) and 2097/98 in ensemble member 071 (CS8) show almost continuous and correlated positive anomalies in daily-mean T and E_S (Fig. S2a, b). In both winters, a notable lack of CAOs is shown which likely enables the persistence of warm temperatures at the surface. Additionally, in CS8 the presence of a surface anticyclone is associated with positive daily-mean T^* and ${E_S}^*$ as well as a lack of P (Fig. S2, orange heatmap). Interestingly, both seasons

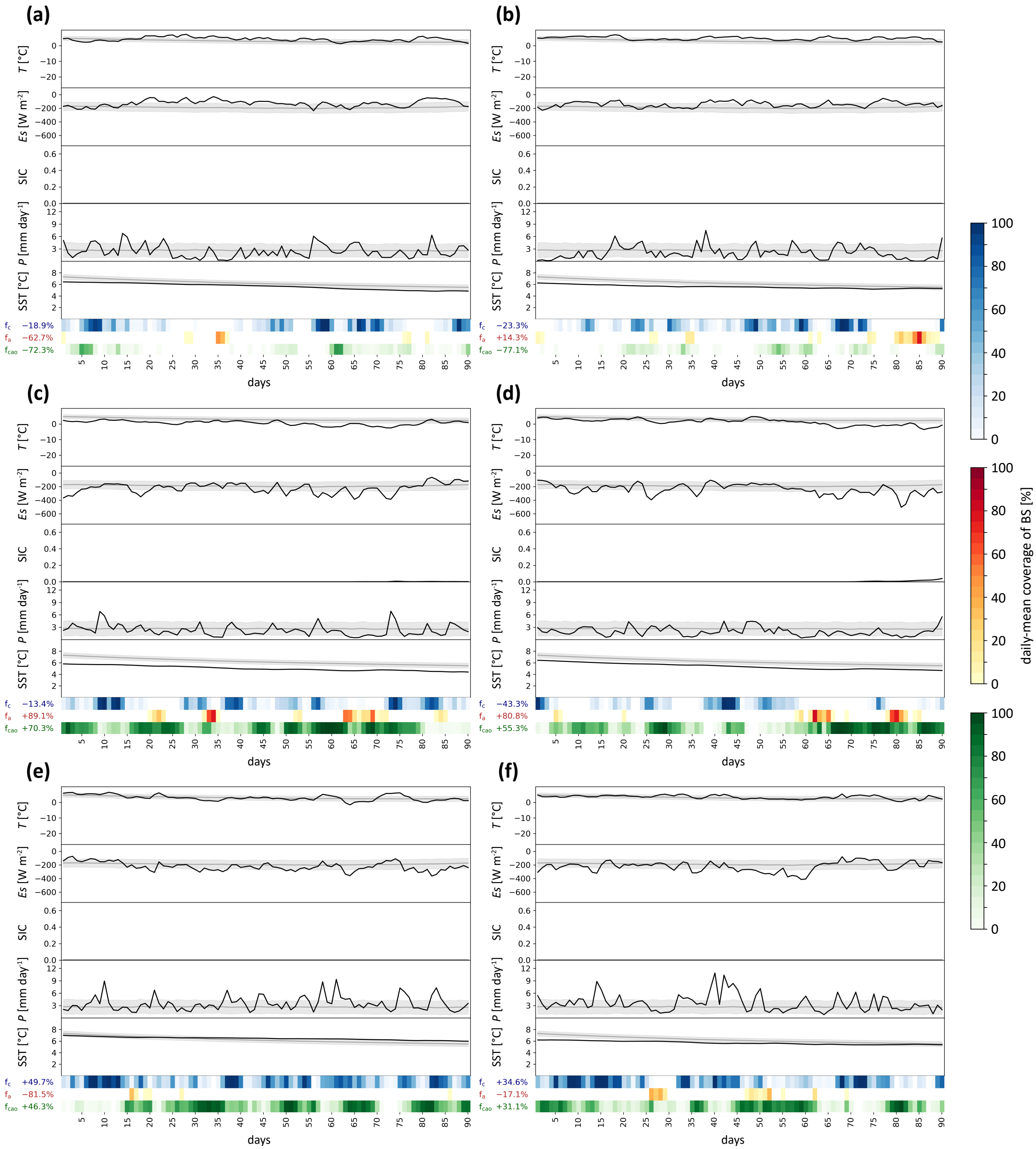

Figure S2. Same as Fig. S1, but for extreme winter case studies in S2100 (a) CS7, (b) CS8, (c) CS9, (d) CS10, (e) CS11, and (f) CS12. Relative seasonally-integrated frequency anomalies of f_c ($f_{c,clim} = 0.31$), f_a ($f_{a,clim} = 0.03$), and f_{CAO} ($f_{CAO,clim} = 0.31$) are given in percentages.

feature slightly colder SST values than usual, which indicates that there is no additional contribution to the maintenance of the warm surface air temperatures by a relatively warm ocean following enhanced SSTs, but that instead the anomalies in both T and E_S are mainly caused by anomalies in the atmospheric circulation. A surface preconditioning in terms of anomalous sea ice coverage at the beginning of a winter season as shown for S2000 simulations is almost impossible in S2100 due to the general absence of sea ice in the BS region.

S2.2.2 Cluster 2: DJF 2091/92 (member 033) and DJF 2092/93 (member 068)

The two chosen case studies, winter 2091/92 in ensemble member 033 (CS9) and winter 2092/93 in ensemble member 068 (CS10), show prolonged periods of strongly negative daily-mean T^* (Fig. S2c, d). Especially CS9 features several periods with T being well below the sigma range. In both winters, the cold episodes can be linked to recurrent CAO events and are possibly maintained by below-average SST values. The frequent CAOs further coincide with episodes of enhanced surface heat fluxes into the atmosphere during both winters, which result in strongly negative daily-mean ${E_S}^*$. In both winters, the occurrence of anticyclones, often during periods with reduced f_c, can be linked to periods with negative daily-mean P^*. While f_a and f_{CAO} are enhanced compared to climatology, particularly DJF 2092/93 features a relative lack in f_c.

S2.2.3 Cluster 3: DJF 2091/92 (member 004) and DJF 2099/00 (member 019)

The analysis of the winters 2091/02 in member 004 (CS11) and 2099/00 in member 019 (CS12) shows several precipitation events throughout these winters, which are further characterized by positive anomalies in both f_c and f_{CAO} (Fig. S2e, f). Apart from short episodes where the BS region is affected by a surface anticyclone, daily-mean P values are almost always above climatology in both winters and are frequently associated with the passage of a cyclone. Several episodes of negative daily-mean ${E_S}^*$ are linked to CAOs, which typically occur with a lag of a few days relative to the passage of a cyclone. This indicates that the respective CAO events are associated with the advection of cold and dry air in the wake of a cyclone.

Similar to S2000, the three clusters show very different characteristics, whereby winters within the same cluster exhibit strong similarities with regard to their substructure, anomalies in weather system frequencies and surface boundary conditions. Winters in cluster 1 feature persistent positive anomalies in T and E_S, which can be linked to the absence of CAO events during most of the season. In contrast, winters in cluster 2 are characterized by prolonged periods where cold conditions and anomalous heat fluxes into the atmosphere prevail, which are associated with recurrent CAOs and the presence of anticyclones in the BS region. Several CAO episodes are similarly characteristic for extremely wet winters in cluster 3, however, these seasons feature an increased cyclone occurrence in BS, which results in negative surface heat flux anomalies and at the same time frequent precipitation episodes.

Although the case studies of S2000 and S2100 cannot be directly compared, it becomes immediately apparent that the climatological conditions in BS change strongly between S2000 and S2100. In S2100, the region becomes ice-free, with SSTs reaching values between +6 °C and +8 °C on average during winter. This is in strong contrast to S2000, when SIC starts to increase from the beginning of December and on average 20 % of BS is covered by sea ice by the end of February (e.g., Fig. S1a, third panel). The absence of sea ice in S2100 is associated with a reduced variability in both T and E_S, which becomes visible in the reduced sigma range of both variables in Figs. S1 and S2. In general, smaller daily-mean anomalies are found for all parameters except P in S2100 compared to anomalies in S2000. However, the anomalies are still comparable relative to the respective climatology, owing to the reduced variability in many surface parameters in BS in a warmer climate. Another interesting result is an overall reduction in the correlation between daily-mean T and E_S values in S2100 (not shown), which is probably linked to the stronger reduction in the variability of T (-66 %) as compared to E_S (-37 %). Next to this reduction in the amplitude and correlation of daily-mean anomalies in T and E_S, we also show similarities in the substructure of winters with similar seasonal-mean anomalies in both S2000 and S2100. For example, negative seasonal-mean anomalies in E_S as shown for cluster 3 in S2000 and clusters 2 and 3 in S2100 are found to be linked to an enhanced occurrence of CAO events. Similarly, persistent warm conditions such as in cluster 1 in both periods feature a pronounced negative f_{CAO} anomaly.

References

Hartmuth, K., Boettcher, M., Wernli, H., and Papritz, L.: Identification, characteristics and dynamics of Arctic extreme seasons, Weather Clim. Dynam., 3, 89–111, https://doi.org/10.5194/wcd-3-89-2022, 2022.